Inversion of Airborne IP data with a multi-mesh approach for parameter definition

Gianluca Fiandaca
Università Statale di Milano
Milan, IT
gianluca.fiandaca@unimi.it

Andrea Viezzoli
Aarhus Geophysics Aps
Risskov, DK
av@aarhusgeo.com

SUMMARY

The interest on Induced Polarization in AEM data (AIP) has significantly increased in recent years, both within the research community and in the industry. However, the inversion of AIP data is particularly ill-posed, especially when spectral modelling, such as Cole-Cole modelling, is used.
In this study we present a novel approach for model space definition, in which the AIP inversion parameters are defined on model meshes which do not coincide with the forward meshes used for data modelling: the link between model and forward meshes is obtained interpolating the model mesh parameters into the forward mesh discretization. This spatial decoupling allows for defining the AIP model parameters, e.g. the Cole-Cole ones, on different model meshes, for instance one for each inversion parameter. In this way, it is possible to define the spectral parameters, like the time constant and the frequency exponent in the Cole-Cole model, on meshes coarser than the resistivity and chargeability ones, vertically and/or horizontally, with a significant improvement in parameter resolution. However, the novel approach is completely general, and allows for incorporating any kind of prior information through the definition of parameters in problem-tailored meshes.
The novel inversion approach is tested on a VTEM AIP survey, highlighting the improvements in model resolution when compared to standard inversion approaches.

Key words: induced polarization, AEM.

INTRODUCTION

The induced polarization (IP) phenomenon in airborne electromagnetic AEM data (AIP) presents a challenge to exploration in many parts of the world. It is a well-known phenomenon and since Smith and Klein (1996) first demonstrate the presence of IP effects, which have been further discussed by several authors (e.g., Marchant *et al.*, 2014; Macnae, 2016; Viezzoli *et al.*, 2017).

IP-affected AEM data are often interpreted in terms of the Cole-Cole model (e.g., Marchant et al., 2014; Viezzoli *et al.*, 2017; Lin *et al.*, 2019), but the inversion problem is particularly ill-posed: for a 1D inversion of a single sounding four parameters have to be retrieved for each model layer.

In this study we present a novel approach for inverting AIP data, in which the inversion parameters are defined on model meshes that do not coincide with the forward meshes used for data modelling: the link between model and forward meshes is obtained interpolating the model mesh parameters into the forward mesh discretization, following the approach presented in Christensen *et al.* (2017). This allows for defining the Cole-Cole spectral parameters, like the time constant and the frequency exponent, on meshes coarser than the resistivity and chargeability ones, vertically and/or horizontally, with a significant improvement in parameter resolution.

The approach is tested on subset of a VTEM survey from central Mexico (the Nieves Silver project, in the state of Zacatecas). Nieves is best characterized as a low-sulfidation epithermal Ag-Au vein within the Mexican altiplano Ag belt. There are a number of world-class Ag deposits within the belt. Veins are hosted in 2-10 m thick shear zones and vein thickness is generally <2 m with sulfide content minor-50% pyrite-stibnite-sphalerite-chalcopyrite-galena. A sulfidation alteration halo surrounds the mineralized shears, containing 2-5% disseminated pyrite. Approximately 200 drillholes have been completed and a resource (indicated & inferred) has been defined within the Central Swarm of 109.9M oz Ag & 116k oz Au @ cut-off grade of 15 g/t (~1/2 oz) Ag.

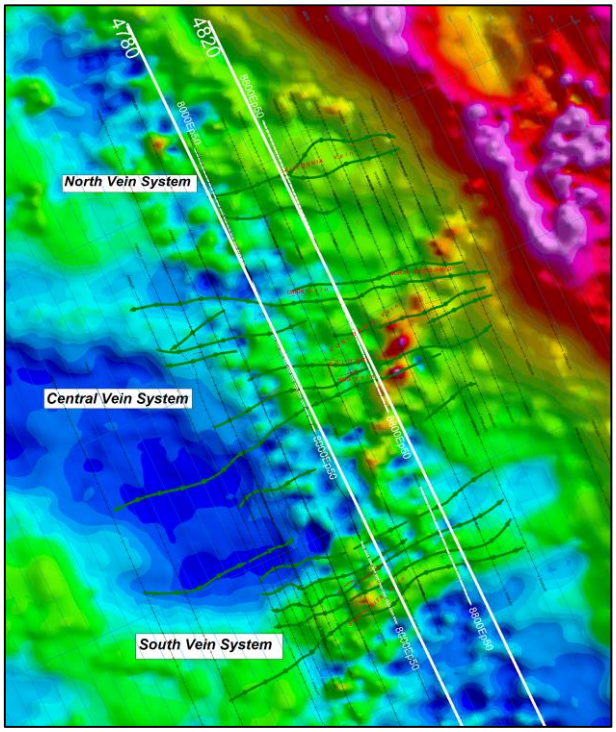

Figure 1. Geophysics survey lines (white), over known and interpreted vein systems (dark green lines) and magnetics background.

A wealth of geophysical methods have been applied at Nieves. They include 1170 line kms of VTEM (2015), 16 lines of CSAMT, 27 lines of ground resistivity and IP, ground magnetics. All the electrical and EM surveys cover the known vein swarms, and extend beyond, in all directions.

Figure 1 shows the subset of the VTEM lines processed with IP, the ground IP lines, the known mineralization, all overlain over the magnetic data.

METHOD AND RESULTS

In the inversion approach presented in this study, the model parameters are defined at the nodes of regular meshes, with constant xy spacings and log-increasing z discretization (Figure 2a). The forward computations are carried out in 1D, through models defined at the sounding positions (Figure 2b), which are linked to the inversion meshes by an interpolation: the parameter values in the forward meshes are defined, layer by layer, interpolating the inversion parameters defined in the model mesh nodes in the centres of the 1D forward layers (Figure 2 c and d).

The interpolation from the parameters $\boldsymbol{P}$ defined on the model mesh nodes into the values $\boldsymbol{p}$ at the forward mesh layers can be expressed through a matrix multiplication, in which the matrix $\boldsymbol{F}$ holds the weights of the interpolation, which depends only on the distances between model mesh nodes and layers of the 1D models at the sounding positions:

$$\boldsymbol{p} = f(\boldsymbol{P}) = \boldsymbol{F} \cdot \boldsymbol{P} \qquad (1)$$

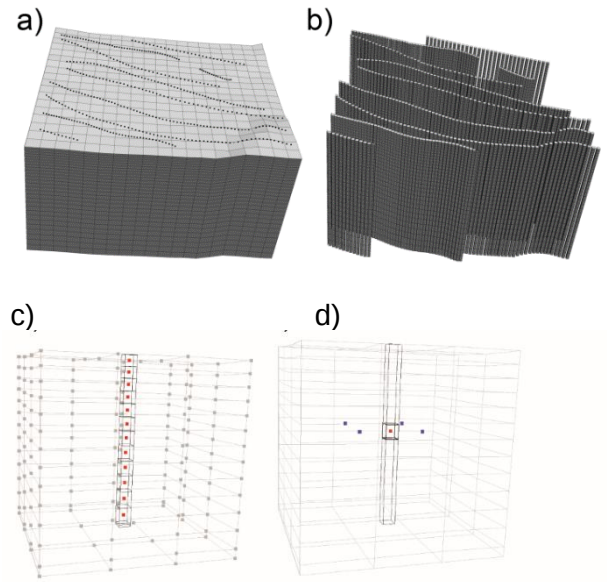

Figure 2. a) Inversion model mesh, with parameters defined at the mesh nodes. b) 1D forward models defined at the sounding positions. The layers of the 1D models are represented as cells with black edges. c) Example of 1D forward model and model mesh nodes. The red dots represent the centres of the layers where the parameters are evaluated through the interpolation (equation 1). d) Example of model nodes (blue dots) contributing to the parameter interpolation in the layer centre (red dot, equation 1).

Consequently, making use of the chain rule for the derivatives, it is possible to express the Jacobian $\boldsymbol{J_P}$ of the data versus the inversion parameters $\boldsymbol{P}$ in terms of the interpolation matrix $\boldsymbol{F}$ and of the Jacobian $\boldsymbol{J_p}$ of the data versus the parameters $\boldsymbol{p}$ defined at the layers of the 1D models:

$$\boldsymbol{J_P} = \boldsymbol{J_p} \cdot \boldsymbol{F}^T \qquad (2)$$

Making use of equations 1 and 2 it is possible to define the Cole-Cole spectral parameters, like the time constant τ and the frequency exponent C, on model meshes coarser than the resistivity and chargeability ones.
The rationale in coarsening the spatial discretization of the spectral parameters is that the sensitivity for τ and C in the 1D models (i.e. the jacobian elements in $\boldsymbol{J_p}$) is relatively small, making their retrieval very difficult and strongly dependent on starting model/constraints when the same spatial discretization of resistivity is used. On the contrary, defining τ and C on coarse meshes, vertically and/or horizontally, increases significantly their sensitivity, and hence their retrieval, without a significant information loss. Indeed, τ and C affect the EM data only in the areas with high chargeability, so that the retrieved value for τ and C will represent the values corresponding to the high-chargeable areas.

We tested the novel inversion approach on the Nieves field examples, which comprises 2114 VTEM soundings acquired along seven parallel lines, approximately 11 km long (Figure 3a). About one third of the soundings present negative late times. The inversion has been carried out with the maximum phase angle (MPA) Cole-Cole reparameterization (Fiandaca *et al.*, 2018), which inverts for the maximum phase φ_{max} of the Cole-Cole model instead of the chargeability m_0, for improved parameter resolution (Lin *et al.*, 2019). We defined the resistivity ρ and the maximum phase φ_{max} on a mesh with 40 m x 40 m horizontal node spacing and 25 layers, with log-increasing depths from 4 m to 400 m (Figure 3b). We used the same horizontal discretization for τ and C, but without any vertical variability (Figure 3c).

The iterative model update $\boldsymbol{m}_{n+1}$ in the inversion is defined as:

$$\boldsymbol{m}_{n+1} = \boldsymbol{m}_n + \left[\boldsymbol{J_P}^T \boldsymbol{C_d}^{-1} \boldsymbol{J_P} + \lambda \boldsymbol{I}\right]^{-1} \boldsymbol{J_P}^T \boldsymbol{C_d}^{-1} \cdot (\boldsymbol{d} - \boldsymbol{f}_n) \qquad (3)$$

where $\boldsymbol{C_d}$ is the data covariance matrix holding the data standard deviations, $\boldsymbol{J_P}$ is the inversion jacobian, $\boldsymbol{d}$ is the data vector, $\boldsymbol{f}_n$ is the forward response of the nth model vector $\boldsymbol{m}_n$ and λ represents the damping.
Table 1 presents a comparison of the sensitivities of the four Cole Cole parameters, in terms of maximum elements of the $\boldsymbol{J_P}^T \boldsymbol{C_d}^{-1} \boldsymbol{J_P}$ matrix, for two cases: 1) no vertical variability for τ and C (i.e. τ and C defined on the mesh of Figure 3c); 2) vertical variability for τ and C (i.e. τ and C defined on the mesh of Figure 3b). Coarsening the spatial discretization of τ and C, allowing no vertical variability, causes an increase in their sensitivity more than ten-fold, with a significant improvement in resolution and decrease in correlations among parameters.

Figure 4 shows the Nieves inversion model, with chargeable bodies in correspondence of the negative AIP data, perfectly fitted as shown in Figure 5.
As mentioned in the introduction, ground IP lines were also acquired on the property. It was a frequency domain survey, measured with a Zonge system, in dipole-dipole configuration (with dipoles both 200 m and 50 m long). Inductive coupling was accounted for with the 3 point method (Coggon, 1984). Figure 6 compares the chargeability obtained from VTEM with the inversion results of the ground IP data (50 m dipole). There is good spatial correlation across the two models, and with Ag concentration from drilling information.

The presented approach is completely general, and allows not only for coarsening the τ and C discretization, but also for incorporating any kind of prior information through the definition of parameters in problem-tailored meshes.

parameter	Max $J_P{}^T C_d{}^{-1} J_P$ value, τ and C **without** vertical variability	Max $J_P{}^T C_d{}^{-1} J_P$ value, τ and C **with** vertical variability
ρ	3.5E+03	3.5E+03
φ_{max}	2.1E+02	2.1E+02
τ	6.5E+01	5.9E+00
C	3.2E+02	1.7E+01

Table 1. Maximum element of the matrix $J_P{}^T C_d{}^{-1} J_P$, for the first iteration of the inversion, without vertical variability for τ and C (Figure 3c) and with vertical variability (Figure 3b).

CONCLUSIONS

We present a novel AIP inversion that decouples the inversion model mesh from the 1D models used in the forward computations. This approach allows for defining the spectral Cole-Cole parameters with coarser spatial discretization, for improved resolution and decreased correlations among parameters. We believe that this will lead to more robust, data-driven AIP inversions that may improve modelling of AIP survey.

ACKNOWLEDGMENTS

The authors would like to thank Joe Inman, Blackberry Ventures, current owners of the Nieves project.

REFERENCES

Christensen, N. K., Ferre, T. P. A., Fiandaca, G., & Christensen, S. (2017). Voxel inversion of airborne electromagnetic data for improved groundwater model construction and prediction accuracy. Hydrology and Earth System Sciences, 21(2), 1321-1337.

Coggon, J. H., 1984, New three-point formulas for inductive coupling removal in induced polarization. Geophysics, 49(3), 307-309.

Fiandaca, G., L. M. Madsen, and P. K. Maurya, 2018, Re-parameterization of the Cole-Cole model for improved spectral inversion of induced polarization data. Near Surface Geophysics, 16, 385–399, doi: 10 .3997/1873-0604.2017065.

Lin, C., Fiandaca, G., Auken, E., Couto, M. A., & Christiansen, A. V. (2019). A discussion of 2D induced polarization effects in airborne electromagnetic and inversion with a robust 1D laterally constrained inversion scheme. Geophysics, 84(2), E75-E88.

Macnae, J., 2016, Quantifying airborne induced polarization effects in helicopter time domain electromagnetics: Journal of Applied Geophysics, 135, 495–502, doi: 10.1016/j.jappgeo.2015.10.016.

Marchant, D., E. Haber, and D. Oldenburg, 2014, Three-dimensional modeling of IP effects in time-domain electromagnetic data: Geophysics, 79, no. 6, E303–E314, doi: 10.1190/geo2014-0060.1.

Smith, R., and J. Klein, 1996, A special circumstance of airborne inducedpolarization measurements: Geophysics, 61, 66–73, doi: 10.1190/1.1443957.

Viezzoli, A., V. Kaminski, and G. Fiandaca, 2017, Modeling induced polarization effects in helicopter time domain electromagnetic data: Synthetic case studies: Geophysics, 82, no. 2, E31–E50, doi: 10.1190/geo2016-0096.1.

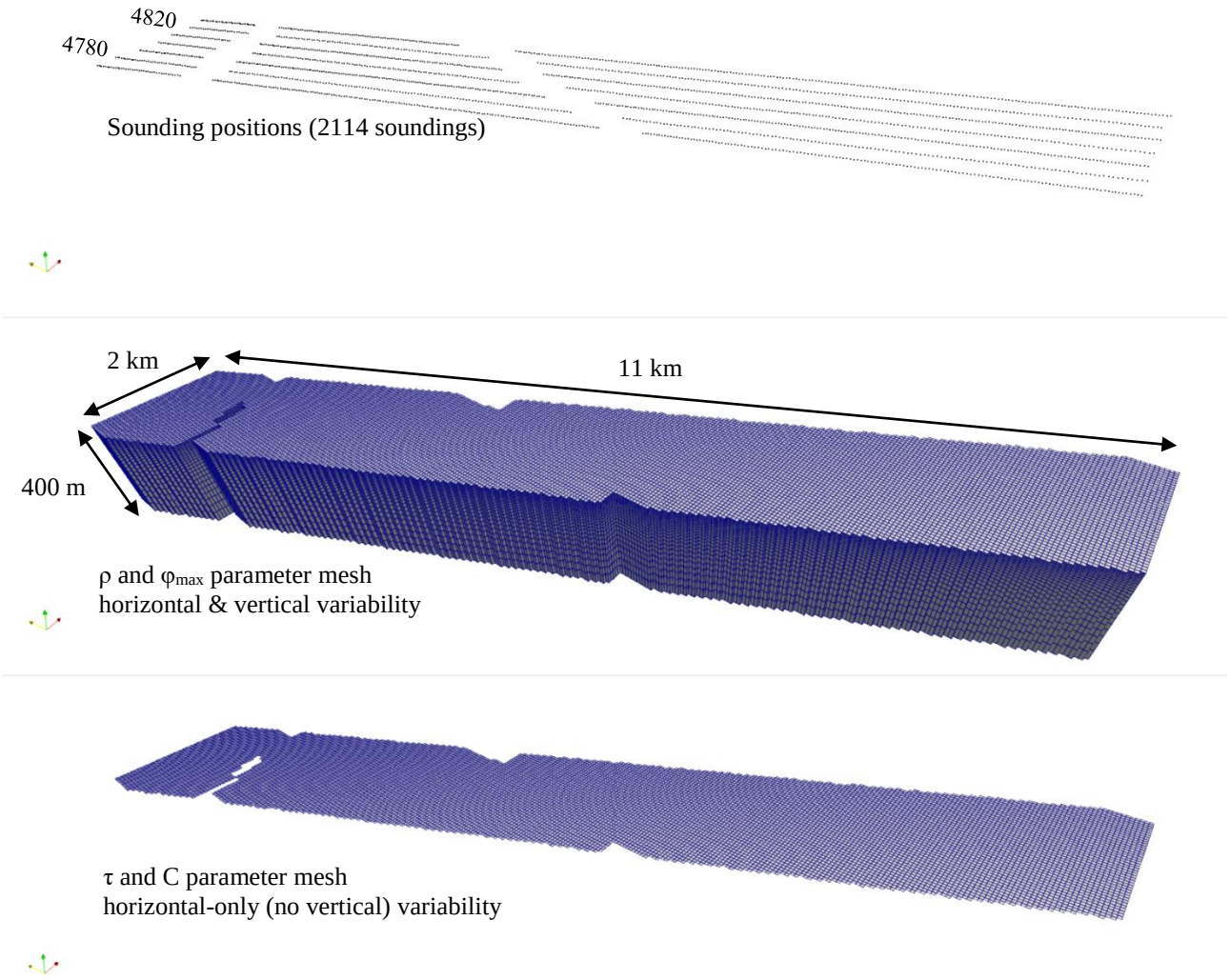

Figure 3. Sounding positions (top) and model meshes for definition of resistivity/maximum phase parameters (middle) and tau/C parameters (bottom).

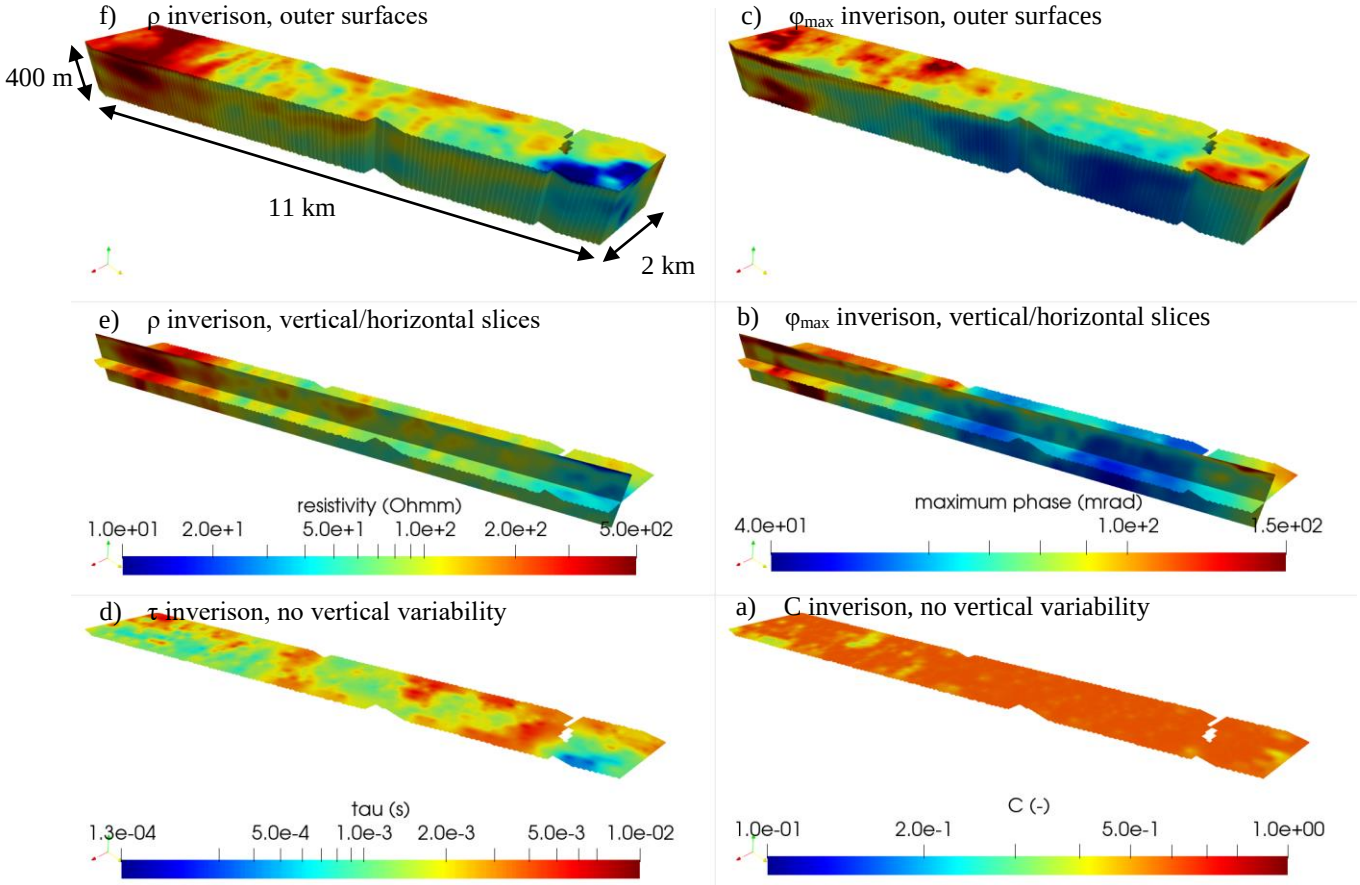

Figure 4. Inversion models. a-b) resistivity inversion model; c) tau inversion model; d-e) maximum phase inversion model; f) C inversion model.

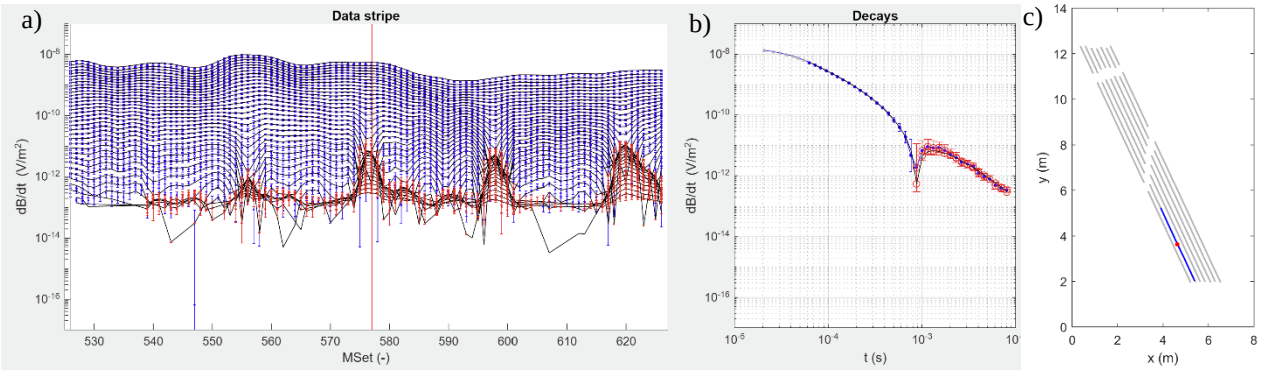

Figure 5 Data fit. a) exemplar data stripe of 100 soundings, with positive data (blue markers), negative data (red markers), data fit (black lines) and position of an exemplar sounding (vertical red line); b) example of sounding fit; c) sounding positions (grey dots), data stripe of subplot a) (blue dots) and highlighted sounding (red dot).

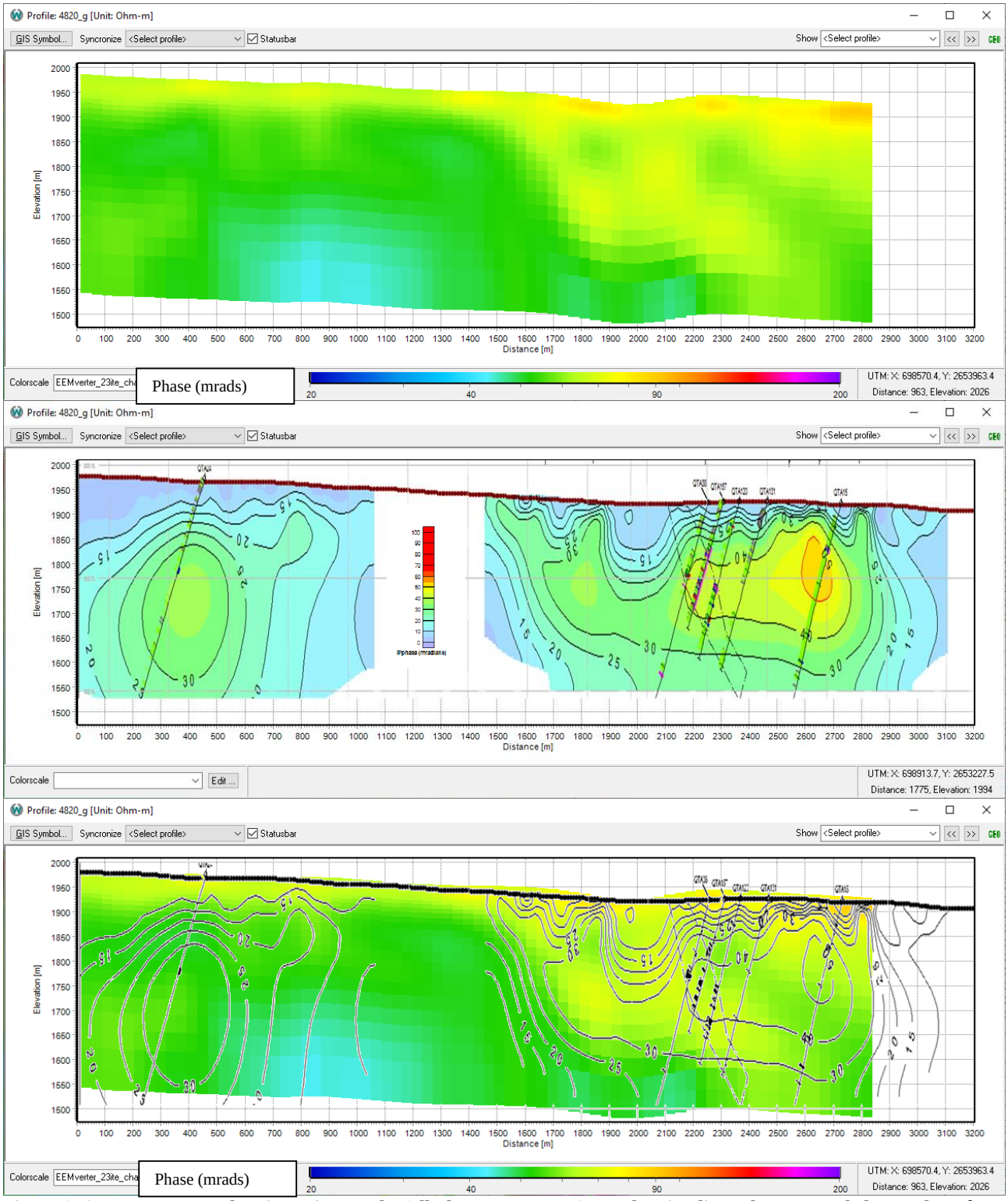

Figure 6. AIP versus ground IP inversion results (all phase parameters), overlapping line. The top panel shown phase from VTEM data, the middle panel from dipole dipole ground IP data, the bottom one overlaps the contours of the ground IP to the background of the AIP. Ag essays from drilling overlay middle and bottom panel.